Determination of Gibbs Energies of Formation of the Ca-Pt-O Compounds from Electromotive Force Method Using CaF_2 as Solid Electrolyte

Hiroyuki Fukuyama, Keiichi Shimizu* and Kazuhiro Nagata*

Institute of Multidisciplinary Research for Advanced Materials
Tohoka University, Sendai 980-8577, Japan
**Department of Chemistry & Materials Science, Tokyo Institute of Technology*
Tokyo 152-8552, Japan

(Received December 26 , 2003;final form January 14, 2004)

ABSTRACT

The standard Gibbs energy changes for the following reactions have been directly determined from electromotive force (EMF) measurements using CaF_2 as the solid electrolyte at elevated temperatures.

$Pt(s) + 4CaO(s) + O_2(g) = Ca_4PtO_6(s)$

$\Delta_r G^\circ$ /kJ = -218.5 + 0.1599T (± 0.3) (1273 - 1313 K)

$Pt(s) + CaO(s) + O_2(g) = CaPtO_3(s)$

$\Delta_r G^\circ$ /kJ = -296.8 + 0.2490T (± 0.6) (1123 - 1173 K)

From the preceding results, the standard Gibbs energies of formation of Ca_4PtO_6 and $CaPtO_3$ have been evaluated as

$\Delta_f G^\circ$ (Ca_4PtO_6) /kJmol^{-1} = -2790.1 + 0.6055 T (± 3.5) (1273 - 1313 K)

$\Delta_f G^\circ$ ($CaPtO_3$) /kJmol^{-1} = -939.7 + 0.3604 T (± 0.88) (1123 - 1173 K).

The phase diagram for the Ca-Pt-O system has been constructed based on the thermodynamic data obtained in the present study.

1. INTRODUCTION

Platinum group metals (PGMs) are widely used for high temperature applications such as electrodes, container materials and catalysis. Recovery processes of used catalysts are currently operated in a pyrometallurgical method using a molten collector metal (copper or iron), or hydrometallurgical methods /1, 2/. Harmful gases such as NO_x and acid solutions emitted from the hydro-process should be suitably treated in a closed process. On the other hand, the pyro-recovery process is well established for dealing with a large amount of PGMs waste without hazardous emissions except for vitreous slag. Therefore, used automotive catalysts are mostly recovered by the pyro-process. However, the recovered PGMs are finally separated to pure metal by hydro-processes. An alternative pyro-separation process, therefore, is required from the environmental point of view.

PGMs react with alkaline earth oxides such as CaO to form intercompound oxides in the specific temperature range. The temperature range and the chemical stability of compounds depend on the kind of PGMs and oxygen partial pressure. For instance, platinum reacts with CaO to form Ca_4PtO_6 and $CaPtO_3$ in air, and the dissociation temperatures of $CaPtO_3$ and Ca_4PtO_6 are 1178 K and 1308 K, respectively /3/. On the other hand, CaO-based iridium compounds such as $CaIrO_3$, Ca_2IrO_4 and Ca_4IrO_6 dissociate at 1408 K, 1443 K and 1513 K, respectively, in air /4/. Thus, taking into account the difference in chemical affinity between PGMs and CaO, PGMs could be separately recovered by pyro-processes using formation and decomposition of the CaO-based compounds. To evaluate the feasibility of such a new pyro-process of PGMs separation, accurate thermodynamic data of the Ca-Pt-O system are essential. However, there is a great lack of reliable thermodynamic data on the Ca-Pt-O ternary system. Only Jacob *et al.* /5/ reported the standard Gibbs energies of formation of Ca_4PtO_6 and $CaPtO_3$ by

electromotive force (EMF) measurements using solid-state cells with Y_2O_3-stabilized ZrO_2 as the electrolyte.

Thus, the present study aims for experimentally determining the Gibbs energies of formation of Ca_4PtO_6 and $CaPtO_3$ with the EMF method using CaF_2 as the solid electrolyte. Based on the results, the equilibrium phase relation for the Pt-Ca-O system is re-established together with quenching experiments.

2. EXPERIMENTAL

Principle

The following fluorine concentration cells were constructed using single crystalline CaF_2 as a solid electrolyte.

(I) Au, O_2, $CaO+CaF_2$ $|CaF_2|$ Ca_4PtO_6 $+CaF_2$, O_2, Pt (II) (1)

(I) Au, O_2, $CaO+CaF_2$ $|CaF_2|$ $CaPtO_3$ $+CaF_2$, O_2, Pt (II) (2)

The transport number of fluoride ion in CaF_2 solid electrolyte is actually unity in the range of temperatures and fluorine chemical potentials used in the present study /6, 7/. The half-cell and overall-cell reactions for cell (1) are represented as follows,

Anode (I):

$$4CaO(s) + 8F^- = 4CaF_2(s) + 2O_2(g) + 8e^- \quad (3)$$

Cathode (II):

$$Pt(s) + 3O_2(g) + 4CaF_2(s) + 8e^- = Ca_4PtO_6(g) + 8F^- \quad (4)$$

Overall:

$$Pt(s) + 4CaO(s) + O_2(g) = Ca_4PtO_6(s) \quad (5)$$

When chemical potentials of oxygen at each electrode are identical, the standard Gibbs energy change of the reaction (5), $\Delta_{r(5)}G^\circ$, can be expressed using the electromotive force, $E_{(1)}$, of the cell and the Faraday constant (9.648531×10^4 $Cmol^{-1}$) as

$$\Delta_{r(5)}G^\circ = -8FE_{(1)} \quad (6)$$

The half-cell and overall-cell reactions for cell (2) are represented as follows,

Anode (I):

$$CaO(s) + 2F^- = CaF_2(s) + 1/2O_2(g) + 2e^- \quad (7)$$

Cathode (II):

$$Pt(s) + 3/2O_2(g) + CaF_2(s) + 2e^- = CaPtO_3(s) + 2F^- \quad (8)$$

Overall:

$$Pt(s) + CaO(s) + O_2(g) = CaPtO_3(s) \quad (9)$$

The standard Gibbs energy change of reaction (9) is related to the EMF, $E_{(2)}$, of the cell (2) by

$$\Delta_{r(9)}G^\circ = -2FE_{(2)} \quad (10)$$

Thermoelectromotive Force

The reference electrode consists of CaO and CaF_2 for both cells (1) and (2). The CaO-CaF_2 system presents a eutectic phase diagram and CaO equilibrates with CaF_2 below the eutectic temperature, 1633 K /8/. To avoid formation of Ca_4PtO_6 (or $CaPtO_3$) at the reference electrodes, a gold wire was used as a lead wire instead of a platinum wire. On the other hand, a platinum wire was used as a lead wire for the sample electrodes, because the sample electrodes must be saturated with platinum. To obtain intrinsic EMF values from the preceding cells, the thermoelectromotive force between platinum and gold lead wires must be subtracted from the total EMF values. The thermoelectromotive force has been experimentally obtained with reference to 273 K prior to the EMF measurements as

$$E_{thermo}/mV = 15.589\text{-}2.56\times10^{-2}T\ (\pm 0.01) \quad (1123\text{-}1313\ K) \quad (11)$$

which agrees well with the theoretical value calculated from the absolute thermoelectric power of platinum and gold /9/.

Sample Preparation

Reagent grade fine powders of $CaCO_3$ (99.5 mass%), Pt (99.5 mass%) and CaF_2 (99.5 mass%) were used. CaO powder was obtained by firing $CaCO_3$ powder at 1273 K in air. A mixed powder of Ca_4PtO_6 and Pt was prepared by heating pressed pellets containing Pt and CaO powders mixed at a molar ratio of 1 : 2.5 in a dry oxygen atmosphere at 1273 K for 1209.6 ks with grinding and repelletization at intervals

of 86.4 ks. A mixed powder of $CaPtO_3$ and Pt was similarly prepared from Pt and CaO powders mixed at a molar ratio of 1.5 : 1 at 1123 K in a dry oxygen atmosphere for 1814.4 ks with grinding and repelletization at intervals of 86.4 ks. The formation of the compounds and the disappearance of the initial CaO were confirmed by X-ray diffraction (XRD) analysis.

The cathode electrode for cell (1) was prepared from an equimolar mixture of (Ca_4PtO_6 + Pt) and CaF_2 powders by compaction at a pressure of 150 MPa to form a cylindrical pellet with a diameter of 10 mm and a thickness of 1 mm. The cathode electrode pellet was sintered under purified oxygen at 1273 K for 43.2 ks to ensure equilibration and mechanical strength before the EMF measurements. The cathode electrode for cell (2) was prepared from an equimolar mixture of ($CaPtO_3$ + Pt) in the same manner except of sintering temperature. The pellet was sintered at 1123 K to avoid dissociation of $CaPtO_3$. The anode electrode was prepared from an equimolar mixture of CaO and CaF_2 with the same procedure with the cathode electrode for cell (1).

Oxygen gas should be completely purified to prevent reactions between CaF_2 in the electrodes and moisture or CO_2. High-purity oxygen gas (99.999 vol%) was further purified by passing it over CuO at 873 K for oxidizing trace level of CO and H_2 to CO_2 and H_2O, respectively. The CO_2 and H_2O gases were removed by passing the oxygen gas through columns containing NaOH, $Mg(ClO_4)$ and P_2O_5. Finally, the gas was purified by passing it through a trap cooled by liquid nitrogen.

EMF Measurements

The cell assembly is illustrated in Figure 1. Single crystalline CaF_2 (diameter 13 mm, thickness 1 mm, OHYO KOKEN KOGYO CO., LTD., Saitama, Japan) was used as solid electrolyte. The CaF_2 solid electrolyte was sandwiched between the cathode and anode electrodes with gold and platinum gauzes (100 mesh, gauze wire diameter 0.07 mm). Gold and platinum lead wires (diameter 0.5 mm) were spot-welded to the gauzes. The cell was spring-loaded to ensure a good contact between electrodes and electrolyte.

After assembling the cell, the cell and thermocouple were placed in the homogeneous temperature region (± 1 K) of the furnace. The alumina reaction tube was evacuated by a rotary pump and filled with the purified oxygen gas. The reaction tube was heated to 573 K, and then the tube was re-evacuated to remove traces of moisture and refilled with the purified oxygen gas. This procedure was repeated three times. After that, the sample was heated to a desired temperature.

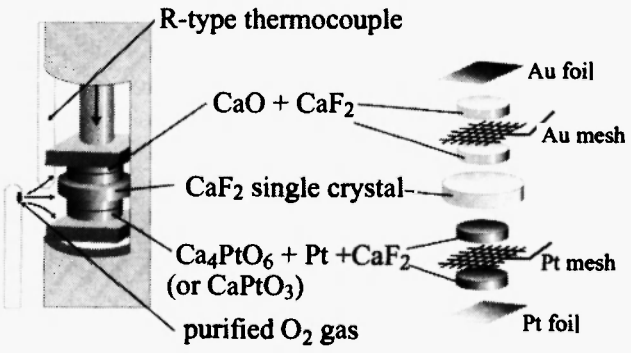

Fig. 1: Schematic diagram of the cell (1) or (2).

The EMF measurements were conducted in the temperature range from 1273 to 1313 K for cell (1) and from 1123 to 1173 K for cell (2) under flowing oxygen at a rate of 100 NmL/min. The temperatures of the cells were measured by a calibrated Pt / Pt-13%Rh thermocouple. The EMF values were measured with a high impedance electrometer (> 10 GΩ). The EMF was considered steady if it was constant within ± 0.1 mV over a period of 7.2 ks. The reversibility of the EMF was checked by passing a small polarization current through the cell in either direction. The EMF values were found to return to their initial values after the passage of current. The EMF was also found to be reproducible by obtaining the nearly equal EMF value on heating and cooling. After the experiment, the electrodes were examined by XRD and it was confirmed that the initial constituents remained throughout the experiment.

Quenching Experiments

On the basis of the thermodynamic results obtained from the EMF studies, the dissociation temperatures of both Ca_4PtO_6 and $CaPtO_3$ can be estimated. To experimentally confirm the dissociation temperatures,

these compounds mixed with a small amount of Pt were fired around the respective dissociation temperatures from 86.4 to172.8 ks. The mixed powders were quenched and subjected to XRD analysis.

3. RESULTS

Figure 2 shows the typical time dependence of the EMF values for cell (1) on changing temperature and passing the small current. The EMF was found to return to the original value after passing the current in 600 s. It should be noted that the EMF values include the thermoelectromotive force between platinum and gold

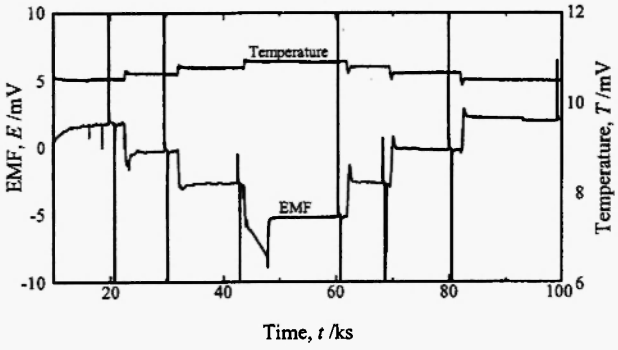

Fig. 2: Time dependence of EMF and temperature of cell (1).

lead wires. The reversible EMF values of the cells (1) and (2) are listed together with the corrected values excluded the thermoelectromotive force in time sequence in Table 1. The corrected values were plotted as a function of temperature in Figures 3 and 4. Data from each run are shown by a separate symbol. Open and solid symbols represent values obtained on heating and cooling, respectively. All data points were subjected to a least-squares fitting, which gives

$$E_{(1)}/\text{mV} = 283.6 - 0.2069T \ (\pm 0.4) \quad (1273\ \text{K} < T < 1313\ \text{K}) \qquad (12)$$

$$E_{(2)}/\text{mV} = 1538 - 1.293T \ (\pm 3) \quad (1123\ \text{K} < T < 1173\ \text{K}) \qquad (13)$$

where the uncertainties are the standard deviations of

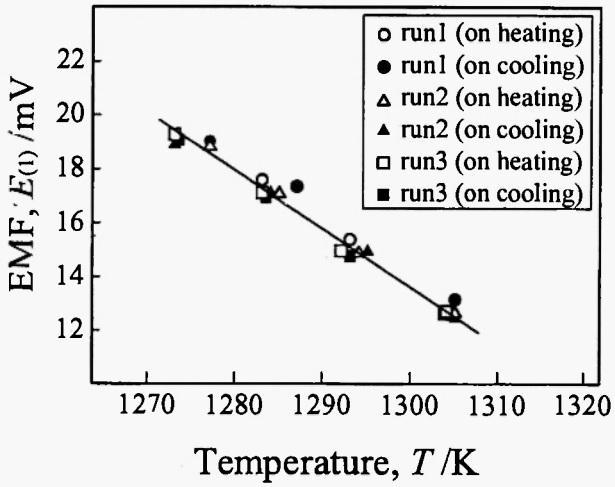

Fig. 3: Temperature dependence of EMF for cell (1).

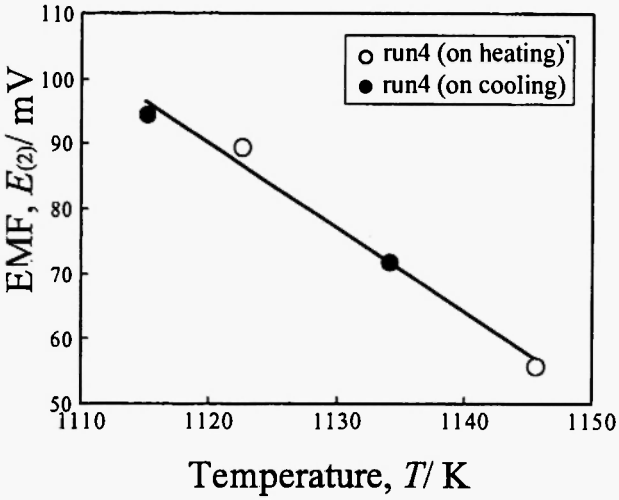

Fig. 4: Temperature dependence of EMF for cell (2).

the scatters in data points. The standard Gibbs energy changes of reactions (5) and (9), $\Delta_{r(5)}G^{\circ}$, $\Delta_{r(9)}G^{\circ}$, are calculated from the EMF values using the equations (6) and (10) as,

$$\text{Pt} + 4\text{CaO} + \text{O}_2 = \text{Ca}_4\text{PtO}_6 \qquad (5)$$

$$\Delta_{r(5)}G^{\circ}/\text{kJ} = -218.5 + 0.1599T \ (\pm 0.3) \quad (1273\ \text{K} < T < 1313\ \text{K}) \qquad (14)$$

$$\text{Pt} + \text{CaO} + \text{O}_2 = \text{CaPtO}_3 \qquad (9)$$

$$\Delta_{r(9)}G^{\circ}/\text{kJ} = -2FE = -296.8 + 0.2490T \ (\pm 0.6) \quad (1123\ \text{K} < T < 1173\ \text{K}) \qquad (15)$$

Table 1
EMF and Standard Gibbs Energy Changes of Reactions (5) and (9) in Time Sequence

Cell (1)

Run	T /K	E /mV	Corrected E /mV	$\Delta_{r(5)}G^\circ$ /kJ
1	1283	0.35	17.59	-13.58
	1293	-2.11	15.38	-11.88
	1305	-4.65	13.15	-10.15
	1287	0.02	17.36	-13.40
	1277	1.95	19.04	-14.70
2	1277	1.84	18.93	-14.61
	1285	-0.21	17.09	-13.19
	1294	-2.64	14.88	-11.49
	1305	-5.15	12.65	-9.77
	1295	-2.60	14.95	-11.54
	1284	-0.15	17.11	-13.21
3	1273	1.92	18.90	-14.59
	1273	2.30	19.28	-14.89
	1283	-0.12	17.12	-13.22
	1292	-2.50	14.97	-11.56
	1304	-5.07	12.71	-9.81
	1293	-2.72	14.77	-11.41
	1283	-0.24	17.00	-13.12
	1273	2.15	19.13	-14.77

Cell (2)

Run	T /K	E /mV	Corrected E /mV	$\Delta_{r(9)}G^\circ$ /kJ
4	1146	42.18	55.89	-10.79
	1134	58.76	72.18	-13.93
	1115	80.87	93.80	-18.10
	1123	76.88	90.02	-17.37

The temperature dependences of $\Delta_{r(5)}G^\circ$ and $\Delta_{r(9)}G^\circ \times 4$ are presented in Figure 5.

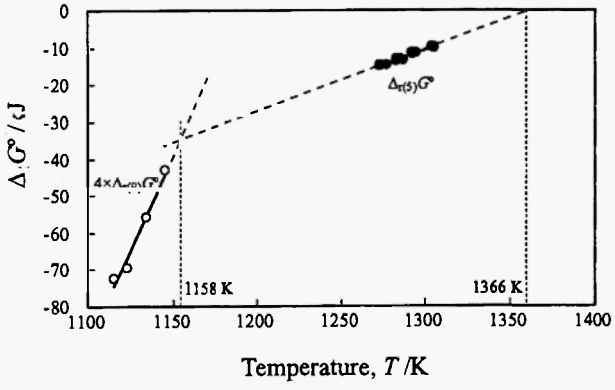

Fig. 5: Standard Gibbs energy changes of the reactions of $Pt+4CaO+O_2 = Ca_4PtO_6$ and $4Pt+4CaO+4O_2 = 4CaPtO_3$.

4. DISCUSSION

Gibbs Energies of Formation of Ca_4PtO_6 and $CaPtO_3$

Using the thermodynamic data of CaO from NIST-JANAF Thermochemical Tables /10/ given by

$$\Delta_f G^\circ (CaO) /kJmol^{-1} = -642.89 + 0.1114T\ (\pm 0.88) \quad (1200\ K < T < 1500\ K) \qquad (16)$$

the standard Gibbs energies of formation of Ca_4PtO_6 and $CaPtO_3$ are evaluated based on the obtained results:

$$\Delta_f G^\circ (Ca_4PtO_6) /kJmol^{-1} = -2790.1 + 0.6055T \ (\pm 3.5) \quad (1273\ K < T < 1313\ K) \qquad (17)$$

$$\Delta_f G^\circ (CaPtO_3) /kJmol^{-1} = -939.7 + 0.3604T \ (\pm 0.88) \quad (1123\ K < T < 1173\ K) \qquad (18)$$

The uncertainty in the Gibbs energy of formation of CaO is caused by the uncertainty in enthalpy of formation of CaO at 298.15 K reported in the thermodynamic tables, which contributes to main part of uncertainties in the $\Delta_f G^\circ$ (Ca_4PtO_6) and $\Delta_f G^\circ$ ($CaPtO_3$).

Jacob *et al.* /5/ determined the $\Delta_f G^\circ$ (Ca_4PtO_6) and $\Delta_f G^\circ$ ($CaPtO_3$) by using solid-state galvanic cells with Y_2O_3-stabilized ZrO_2 as an electrolyte. They are smaller than the present values by 7 kJ for Ca_4PtO_6 and 15 kJ for $CaPtO_3$. The difference in the Gibbs energy of formation causes the large discrepancy in dissociation temperatures of both Ca_4PtO_6 and $CaPtO_3$, which is explained in the next section.

Phase Diagram of the CaO-(Pt+O_2) system

According to the phase relations in the CaO-Pt system in air reported by McDaniel /3/, $CaPtO_3$ decomposes into (Ca_4PtO_6+Pt), and Ca_4PtO_6 decomposes into (CaO+Pt) at respective dissociation temperatures. The dissociation temperatures can be estimated from the present results. Figure 5 illustrates that the two lines of $\Delta_{r(5)}G^\circ$ and $\Delta_{r(9)}G^\circ \times 4$ intersect each other at 1158 ± 3 K. At the temperature of the intersection, the standard Gibbs energy change of the following reaction is equal to 0.

$$4CaPtO_3(s) = Ca_4PtO_6(s) + 3Pt(s) + 3O_2(g) \qquad (19)$$

In other words, $CaPtO_3$, Ca_4PtO_6 and Pt are in equilibrium at 1158 ± 3 K under the oxygen partial pressure of 1 bar, which corresponds to the dissociation temperature of $CaPtO_3$ under oxygen partial pressure of 1 bar. The dissociation temperature of Ca_4PtO_6 is given by the temperature that $\Delta_{r(5)}G^\circ$ is equal to 0, which is 1366 ± 2 K under oxygen partial pressure of 1 bar as presented in the figure.

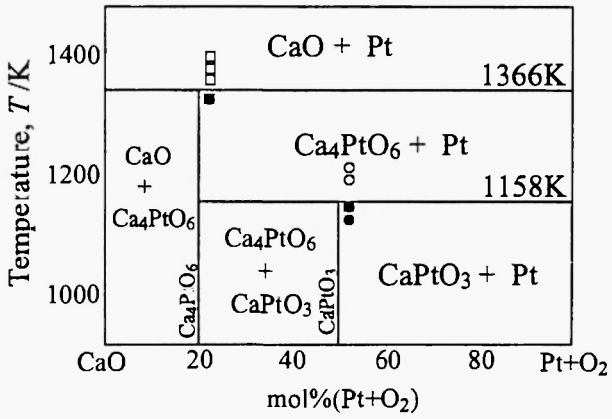

Fig. 6: Phase diagram for the CaO-(Pt+O_2) system under oxygen partial pressure of 1 bar together with the results of the quenching experiments. ●: $CaPtO_3$ was stable, ○: $CaPtO_3$ decomposed into Ca_4PtO_6 and Pt, ■: Ca_4PtO_6 was stable, □: Ca_4PtO_6 decomposed into CaO and Pt.

Figure 6 shows the phase diagram of the pseudo-binary CaO - (Pt+O_2) system estimated from the above discussion. The results from the quenching experiments are also presented in the figure. Solid circles and squares represent that $CaPtO_3$ and Ca_4PtO_6, respectively, are stable. Open symbols represent that the respective compounds decomposed at the temperatures. The estimated dissociation temperatures agree with the results from the quenching experiments.

On the other hand, the dissociation temperatures calculated from the results obtained by Jacob *et al.* /5/ are 1406 K for Ca_4PtO_6 and 1265 K for $CaPtO_3$, which are much higher than the present results and inconsistent with the results from the quenching experiments. Thus, the present results disagree with the results obtained by Jacob *et al.* However, Jacob's results agree well with the phase relations determined in air by McDaniel /3/. The reason for the contradiction is not clear at the moment.

5. CONCLUSIONS

The standard Gibbs energy changes for the following reactions have been directly determined from electromotive force (EMF) measurements using CaF_2 as

the solid electrolyte at elevated temperatures.

$Pt(s) + 4CaO(s) + O_2(g) = Ca_4PtO_6(s)$
$\Delta_r G^\circ$ /kJ = -218.5 + 0.1599T (± 0.3) (1273 - 1313 K)

$Pt(s) + CaO(s) + O_2(g) = CaPtO_3(s)$
$\Delta_r G^\circ$ /kJ = -296.8 + 0.2490T (± 0.6) (1123 - 1173 K)

From the results, the standard Gibbs energies of formation of Ca_4PtO_6 and $CaPtO_3$ have been evaluated as

$\Delta_f G^\circ (Ca_4PtO_6)$ /kJmol^{-1} = -2790.1 + 0.6055 T (± 3.5)

$\Delta_f G^\circ (CaPtO_3)$ /kJmol^{-1} = -939.7 + 0.3604 T (± 0.88).

The phase diagram for the Ca-Pt-O system has been constructed based on the thermodynamic data obtained in the present study. The dissociation temperatures of Ca_4PtO_6 and $CaPtO_3$ under oxygen partial pressure of 1 bar are 1366 ± 2 K and 1158 ± 3 K, respectively.

ACKNOWLEDGMENTS

This research was supported by a Grant-in-Aid for Scientific Research from the Japan Society for the Promotion of Science (JSPS).

REFERENCES

1. J. E. Hoffmann, *J. Metals*, **43**, 40-44 (1988).
2. M. Benson, C. R. Bennet, J. E. Harry, M. K. Patel and M. Cross, *Resources, Conservation and Recycling*, **31**, 1-7 (2000).
3. C.L. McDaniel, *J. Am. Ceram. Soc.*, **55** (8), 426-427 (1972).
4. C.L. McDaniel and S. J. Schneider, *J. Solid State Chem.*, **4**, 275-280 (1972).
5. K. T. Jacob, T. H. Okabe, T. Uda and Y. Waseda, *Z.Metallkd.*, **90** (7), 491-498 (1999).
6. V.A.Levitski, *J. Solid State Chem.*, **25**, 9-22 (1952).
7. J. Delcet, R. J. Heus and J. J. Egan, *J. Electrochem. Soc.*, **125** (5), 755-758 (1978).
8. A. K. Chatterjee and G. I. Zhmoidin, *J. Mater. Sci.*, **7** (1), 93-97 (1972).
9. K.-H. Hellwege and O. Madelung, *Landolt-Börnstein, Numerical Data and Functional Relationships in Science and Technology, New Series, Group III: Crystal and Solid State Physics, Volume 15, Metals: Electronic Transport Phenomena, Subvolume b*, Springer-Verlag Berlin, 48-64 (1985).
10. M. W. Chase, Jr., *NIST-JANAF Themochemical Tables, Forth Edition Part I, Al-Co*, American Chemical Society and the American Institute of Physics for the National Institute of Standards and Technology, New York, 729 (1998).